sustainability

MDPI

Article

Spatial Pattern of Carbon Sequestration and Urban Sustainability: Analysis of Land-Use and Carbon Emission in Guang'an, China

Zhigang Li [1,2], Jialong Zhong [3,*], Zishu Sun [3] and Wunian Yang [1,3]

1 Key Laboratory of GeoSpatial Information Technology of Ministry of Land and Resources, Chengdu University of Technology, No. 1 Dongsan Road, Erxian Bridge, Chenghua District, Chengdu 610059, China; cdlglzg@163.com (Z.L.); ywn@cdut.edu.cn (W.Y.)
2 College of Management Science, Chengdu University of Technology, No. 1 Dongsan Road, Erxian Bridge, Chenghua District, Chengdu 610059, China
3 College of Earth Sciences, Chengdu University of Technology, No. 1 Dongsan Road, Erxian Bridge, Chenghua District, Chengdu 610059, China; cdlgszs@163.com
* Correspondence: jialogn@gmail.com

Academic Editor: Jianguo (Jingle) Wu
Received: 31 July 2017; Accepted: 23 October 2017; Published: 26 October 2017

Abstract: The state of the urban carbon cycle is an important indicator for managing fossil energy consumption and land resources and it is also a basis for the planning of urban eco-services and urban sustainable development. This paper aims to analyze the spatial distribution of the carbon cycle of the mono-centric cities, based on the von Thünen concentric ring theory, using the InVEST (Integrated Valuation of Ecosystem Services and Trade-offs) model and an atmospheric diffusion model to assess the carbon sequestration capacity of land cover/use, to estimate carbon emissions, discuss influencing factors that determine changing trends in carbon sequestration capacity and to predict the changing law of the carbon sequestration eco-service spatial pattern based on scenario simulations. The results of this study show: (1) In Guang'an, the spatial distribution of the carbon cycle follows a concentric ring pattern. From the concentric ring pattern center, the first annular zone represents the carbon emissions, which lie at the concentric ring center; the second annular zone represents the carbon sequestration service; and the third annular zone represents stable carbon stock; (2) The structure of the concentric ring has not changed, but the spatial distribution of carbon sequestration and carbon density has changed due to fossil energy consumption and land cover/use change. From 2014 to 2016, the carbon emission zone shrunk, while the carbon sequestration service zone expanded and the carbon density increased—the increase of forest land is the main factor in the increase of carbon density; (3) The current carbon sequestration eco-service in Guang'an is not the best development condition. The planning of urban eco-service spatial patterns and land cover/use should consider the protection of cultivated and ecological areas at the same time. The results of this study can help the government implement spatial planning and regional policy interventions for land cover/use and eco-service.

Keywords: urban sustainable development; carbon sequestration eco-service capacity; spatial distribution of carbon cycle; carbon emission; land cover/use; scenario simulation

1. Introduction

The urban carbon cycle is a component of the global carbon cycle [1]. In China, urban expansion has increased energy consumption and carbon emissions [2]. Carbon sequestration capacity—the process, activity, and mechanism for removing carbon dioxide from the air—not only refers to the

amount of carbon dioxide forests and soils can capture and store, but also to the amount of organic carbon soil can store. The carbon sequestration capacity of densely populated cities is limited, so those cities must transfer the ecological pressure of carbon sequestration to the suburbs [3]. Urban suburbs have a close ecological relationship with cities [4,5]. The creation of urban ecological zones should involve the consideration of ecological security [6]. The division of the study area into ecological functional units can help to allocate ecosystem resources [7] and reveal ecological and environmental problems [8].

This paper focuses on the spatial distribution of the carbon cycle in cities which can be regard as mono-centric area in a large spatial scales, with relatively low degree of urbanization (mono-centric cities have small human populations, undeveloped transportation systems, and relatively minor industrial production activity). Manoratna et al. described the actual traffic flow along one major intra-urban corridor using a mono-centric city model [9]. Li et al. found that planned employment decentralization may help resolve the traffic congestion of a city with a mono-centric structure [10]. Salvati and Carlucci used the mono-centric city model to analyze urban morphology and land use changes [11]. Those studies represented that the distribution of geographic features of mono-centric city will be radial pattern. In other theories, the von Thünen model is also related to the spatial pattern of urban features. The von Thünen concentric ring model is the most famous model of regional structure, with a single urban market center [12]. Von Thünen studied how the height and slope of the rent curve for different land uses depend on the distance from the center [13]; that is, determine the rent through the distance from the urban commercial center, which formed the agricultural land use of the von Thünen ring structure. In von Thünen's own words: "if this use is chosen with the utmost rationality, what kind of agriculture will develop and how will the distance to the city affect the use of land" [14]? Angelsen presented a framework for analyzing the tropical deforestation and reforestation based on the von Thünen model, and associated the forest transition (FT) theory, to study changes in forest cover over time [15]. Kitsikopoulos analyzed the relationship between urban demand and agrarian productivity by the von Thünen model [16]. Many studies depicted the impact of land cover/use changes on carbon sequestration service without considering the spatial pattern. Human activities have changed the land cover/use type and directly impacted urban carbon sequestration. Urban development, increased demand for construction land, and urban expansion are major factors reducing regional carbon sequestration capacity [17]. Land cover/use changes, caused by human activity, directly affect soil carbon and the carbon cycle [18]. Change of land cover/use types affects carbon emissions and carbon sequestration [19]. Forests and grasslands are typical land cover types possessing strong carbon sequestration capacity [20]. Green areas in cities capture and store relatively small amounts of the carbon emissions from human activities [21,22]. This issue has been discussed; however, no studies depict carbon sequestration service by integrating LUCC and the von Thünen model. This paper therefore surveys the situation with land cover/use and carbon emissions, and processes and evaluates the data on land-use and carbon emissions. We studied the Gang'an area and developed a method for recognizing the distinct characteristics of carbon sequestration and the spatial distribution of those characteristics. We then analyzed the effects of land cover/use on carbon sequestration and its spatial evolution. This study provides a scientific basis for developing low carbon policies and planning for urban or rural land. Mancebo and Salles agree that it is meaningless to talk about urban sustainability if we stop at the city limits and that sustainable urban policies should consider an urban–rural continuum [23]. Therefore, we take into account a region that has expanded in all directions beyond the urban administrative boundaries.

The main purposes of the simulation of land cover/use changes are to visualize the trends in those changes under different policies and to provide reference information for the modification of government strategy [24]. It is helpful to investigate the mechanism of land cover/use changes and even to optimize land cover/use allocation for sustainable development [25]. By simulating land cover/use changes under different total factor productivity (TFP) scenarios, Luo depicted land cover/use competition in socio-economic development and the protection of environment [26].

Based on simulations of land cover/use using land use planning scenarios, natural development scenarios, ecological-oriented scenarios and farmland protection scenarios, and comparing them with local situations, one study depicted the driving factors of land use [27]. Thus, the simulation of scenarios is used in this study to elucidate the impact of land cover/use changes on the carbon cycle spatial distribution, and the results can be used to support the formulations of land cover/use.

A generally-accepted definition of urban sustainability is lacking. Taking ecosystem and human well-being into account, urban sustainability can be defined as an adaptive process of facilitating and maintaining virtuous cycle between ecosystem services and human well-being through concerted ecological, economic, and social action response to changes within and beyond the urban landscape [28–30]. Urban sustainability is closely associated with ecosystem services and their relationship to society; Nassauer et al. concluded that it is possible to promote urban ecosystem service through urban sustainability planning [31]. However, a city that derives most of its ecosystem services from other regions, nationally or internationally is subject to myriad environmental and sociopolitical uncertainties, thus is hardly sustainable in the long run [32]. Thus, timely and effective assessments of the changes of regional ecosystem services are an important issue in the fields of urban ecology and sustainability science [33]. Therefore, no matter which aspect of urban sustainability is being studied, ecosystem service function, environment and urban landscape pattern are the important parts of urban Sustainable development.

Guang'an is a typical mono-centric spatial structure city, similar to other mono-centric cities in China. The actual city area is small, with sparse internal vegetation. The main park is located on the urban edge, and the ecosystem carbon sequestration capacity of the city is minimal. Increasing population and industrial development have hastened the expansion of housing and commercial construction and the city's carbon sequestration capacity has decreased significantly. In line with the current urban development trend, local government has implemented policies to reduce emissions and return the farmland to forest, which are helpful for restoring the ecosystem. However, certain ecological and environmental management issues remain.

(1) The urban ecological land is distributed between three administrative regions of Guang'an, thus the carbon pool is scattered across these three administrative areas, which is a problem for unified management.
(2) From the projection of land cover/use, the administrative boundary has broken the integrity of the ecological system. The boundary between the ecological systems and the administrative divisions is inconsistent, which affects government management of the ecological environment. All of the administrative regions need to coordinate efforts to address the combined problems of ecological services and sustainable urban development.
(3) There is a lack of ecological and land cover/use data analysis at the local level. Verification of regional land cover/use planning and policies would be useful.

In this study, we attempted to address the following questions: (1) Does the spatial distribution of carbon cycle modeling follow the von Thünen model? (2) If so, what is the spatial distribution pattern? (3) What are the differences in spatial distribution for different possible land cover/use scenarios?

2. Materials and Methods

2.1. Study Area

Guang'an (Figure 1) is a fourth-tier city with economic development that is dependent on local small and medium enterprises or resource enterprises; residents with increasing spending power; and a relatively slow development rate. The geographical coordinates are 30°01′–30°52′ N, 105°56′–107°19′ E. The E–W span is 134.5 km and the N–S span is 93.6 km. Total area is 634,400 ha. The geographical impact on urban development is small. The development of fourth-tier cities fits a mono-centric city development model [5,34]. Fourth-tier cities play an important role in the township development

of China. More and more populations and industries appear in these cities, putting more pressure on the urban ecology. The local government has been working on greening and emission reduction, such as the program of City Forest and Seedling Base Construction [35]. Based on the China Statistical Yearbook and Guang'an Statistical Yearbook, per capita forest occupancy of Guang'an is 0.0556 million hectares in 2015, while it is 0.1511 million hectares for China [36,37]. The eco-management in Guang'an remains a challenge. In Figure 1, the large circle represents the study area, with the center being the urban gravity center, according to the von Thunen model [16,38].

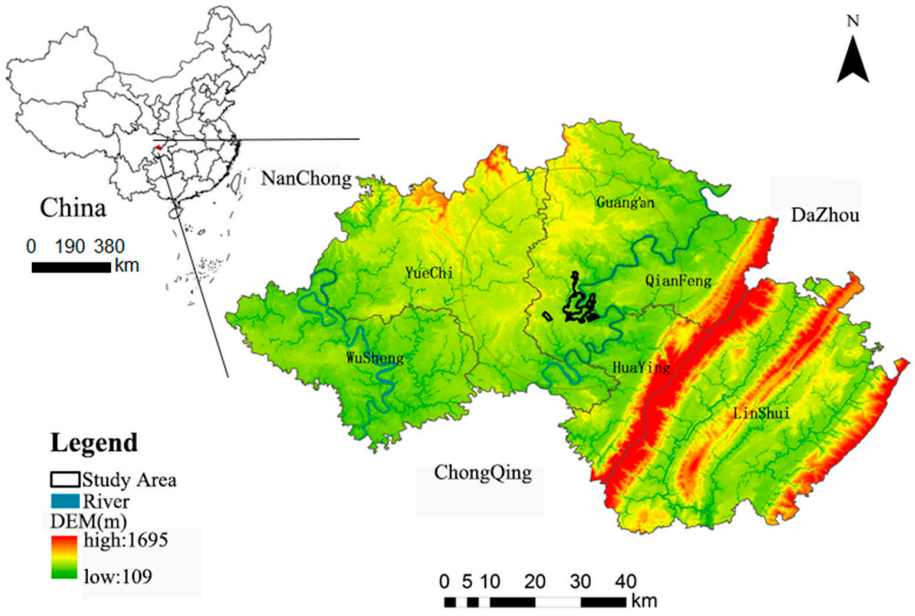

Figure 1. Guang'an study area.

2.2. The Spatial Distribution of Carbon Sequestration Eco-Service

2.2.1. InVEST Model

We used the InVEST model from ecosystem service models to calculate carbon stocks. The carbon pool of InVEST, similar to IPCC (Intergovernmental Panel on Climate Change) Guidelines, contains aboveground biomass (C_{above}), belowground biomass (C_{below}), dead organic matter biomass (C_{dead}), and soil biomass (C_{soil}). This model is a distributed algorithm based on "3S" technologies, which overcome the limitations of traditional methods and provide a novel technical method for the spatial expression, dynamic analysis, and quantitative assessment of ecosystem service function [39,40]. The InVEST model is among the most useful ecosystem evaluation models [41]. The carbon module in InVEST3.3.3 [42] employs LUCC layers, wood harvest rates, harvested product degradation rates, and the carbon density of four carbon pools to assess carbon stocks of the general landscape. InVEST considers that it is difficult, in most cases, to accurately measure carbon density due to data qualification. Because of this, it allows direct user input of carbon density and reduces the inaccuracy produced by other inputs. To use this function, we chose the "uncertainty analysis pattern" when running the carbon module, and input the grid map of land cover/use change and the parameter table of carbon density. The outcome of the carbon module was a grid map, and the pixel value was the carbon stocks of the pixel.

We used the remote sensing data of Landsat 8 on 6 August 2014 and 11 August 2016 [43] to get land cover/use data of 30 m resolution by ENVI5.3 platform with WGS84 coordinate system, UTM projection and maximum likelihood imagery classification. These data are input into InVEST, and the carbon pool density data required by InVEST were mainly summarized from other papers [44–46].

2.2.2. The Spatial Distribution

The carbon density data output by InVEST have the same accuracy as the land cover/use data, and present the detailed information of carbon stocks, but cannot show the distribution pattern of carbon sequestration. This can be solved by sampling and interpolation using spatial analysis tool [47,48].

2.3. Atmosphere Diffusion Simulation Model

2.3.1. Carbon Emissions and Atmosphere Diffusion Simulation Model

The carbon emissions in urban carbon cycle from the fossil fuel burning [49,50] were calculated using statistical energy consumption data. The data were compiled from the official statistics released by Guang'an Bureau of Statistics. Based on "the Regional GDP Energy Consumption Statistics Yearbook of States and Municipalities", Guang'an ranks third on the production of a unit of GDP per unit of energy consumption (first and second are Pan'zhi'hua City and Da'zhou City, respectively) in Sichuan Province.

Zhang Renquan [51] found that the Gaussian atmospheric diffusion model reflects the carbon emissions in wind. By querying the Meteorological data in Guang'an, the wind speed is 0.3–0.5 m/s, so the Small Quiet Breeze Spread Model was appropriate [43]. Its mathematical expression is

$$c(x,y) = 2Q/\sqrt{(2\pi)^3\gamma_{02}\eta^2}\cdot\exp\left(u/2\gamma_{01}^2\right)$$
$$\left\{1+\sqrt{2\pi}\cdot S\cdot\exp\left(S^2/2\right)\cdot[\phi(S)-\phi(S-W)]-\exp\left(SW-W^2/2\right)\right\}. \quad (1)$$

Here, $\eta^2 = x^2+y^2+u^2t_0^2+2xut_0+(\gamma_{01}^2H_0^2)/\gamma_{02}^2$, $S = xu+(u^2t_0)/(\gamma_{01}\eta)$,

$$t_0 = \sqrt[3]{a_xa_ya_z/\gamma_{01}^2\gamma_{02}}/4.3, \phi(S) = 1/\sqrt{2\pi}\int_{-\infty}^{s}\exp\left(-t^2/2\right)dt,$$

$$\gamma_{01} = \sigma_x/(T+t_0), \gamma_{02} = \sigma_z/(T+t_0), W = \eta/(t_0\gamma_{01}).$$

$c(x,y)$ represents the concentration of pollutants (mg/m^3) at any point (x,y) of the ground; σ_x and σ_z represent the diffusion parameters (m) of the contaminant clusters in the x and z directions; the z axis is in the vertical direction; Q represents the amount of pollutant discharged (mg/s) per unit time; u represents the average wind speed (m/s) at the height of the pollutant discharge point; t represents the running time (s) after the smoke residue formed by the pollutant leaves the discharge port; H_0 represents the effective discharge height of the pollutant (m); γ_{01} and γ_{02} represent the regression coefficients of horizontal and vertical diffusion parameters (m/s); a_x, a_y, and a_z represent the width of the source in the x, y, and z directions; and t_0 represents the initial time of the formation of the source.

The model parameters were modified slightly. The initial time of CO_2 gas is not formed when the CO_2 gas is discharged, but immediately after the gas is generated, so $t_0 = 0$ is substituted into Equation (1)

$$c(x,y) = 2Q/\sqrt{(2\pi)^3\gamma_{02}\eta^2}\cdot\exp\left(-u/2\gamma_{01}^2\right)\left\{1+\sqrt{2\pi}\cdot S\cdot\exp\left(S^2/2\right)\cdot\phi(S)\right\}. \quad (2)$$

In the windy wind model, we suppose that x has the same effect as the diffusion in the y direction, i.e., $\sigma_x = \sigma_{zx} = \sigma$, and ignore the diffusion height ($H_0 = 0$), thus we get $\gamma_{02} = \gamma_{01} = \gamma$, $\eta^2 = 2x^2$, and $S = \sqrt{2}\gamma/u$, $\gamma = x/\sigma u$, which were substituted into Equation (2):

$$C(x,y) = Q/\sqrt{(2\pi)^3\gamma_{02}\eta^2}\cdot\exp\left(-x^2/2\sigma^2\right)$$
$$\left\{1+\sqrt{2\pi}\cdot\left(x/\sqrt{2}\sigma\right)\cdot\exp\left(x^2/4\sigma^2\right)\cdot\phi\left(x/\sqrt{2}\sigma\right)\right\}. \quad (3)$$

To facilitate the calculation, let $K = 1 + \sqrt{2\pi} \cdot \left(x/\sqrt{2}\sigma\right) \cdot \exp\left(x^2/4\sigma^2\right) \cdot \phi\left(x/\sqrt{2}\sigma\right)$, thus Equation (3) can be written as

$$c(x,y) = Q/\sqrt{(2\pi)^3 \gamma_{02} \eta^2} \cdot \exp\left(-x^2/2\sigma^2\right) \cdot K. \quad (4)$$

2.3.2. The Spatial Logical Location for the Urban Carbon Sources

C diffusion from a carbon source is in the atmospheric dispersion category, and there are numerous carbon sources in the study area. The organized energy consumption data are based on annual time scales. In this study, we considered the regions with large city carbon emission as carbon sources, and replaced the distribution pattern of total C emissions with the C distribution model of these regions.

POI (Point of Information) data contain the name, location and other information. POI for more intensive areas is considered as the higher commercialization degree, while more intensive industrial areas are the core areas of carbon emissions. Therefore, we used the point with the highest POI density as a substitution point for the urban carbon source. The density of urban POI was taken as the substitution point of urban carbon source, and the density of POI was calculated by the point density tool in ArcGIS.

2.4. The Spatial Distribution of Carbon Cycle

2.4.1. Assumption

Based on the description in von Thünen model of the distribution of the land cover/use features in cities and suburbs, during urban expansion, and the way that a city gets its surrounding natural resources, we assumed that the land cover/use types with high carbon density distributed as concentric ring pattern between urban area and farmland, and the carbon emissions of urban carbon sources also surround the city as ring pattern. Therefore, the spatial distribution of carbon cycle resembles the following in Figure 2: Zone I is Carbon Emission Zone; Zone II is Carbon Sequestration Zone, where urban land use is interspersed with urban green cover; and Zone III is Stable Carbon Stock Zone, where farmland is the main land use types. Zone III is far away from carbon source, the impact of human activity is relatively weaker, and carbon density is stable.

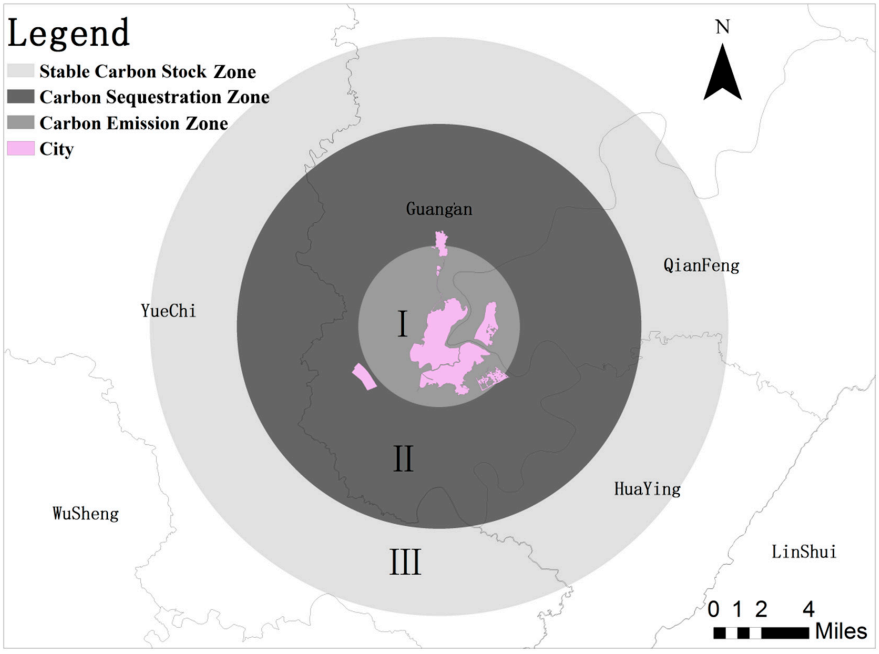

Figure 2. The range of carbon sequestration zone of Guang'an.

2.4.2. The Subdivided Inner Rings

City development can be viewed as the progress of expanded urban concentric ring pattern. A ring structure is the basic spatial structure of a city [52]. The simplest urban concentric ring pattern is divided into three rings. The inner ring mainly includes the core developed area. The transition ring is the transition region of city to village, and the agriculture-based outer ring [53]. According to the extent of non-agricultural area, population structure, and economic development, urban concentric ring pattern is divided into a central area, an edge area, and a peripheral area [54]. Jiang and Zhang [53] divided this structure into three rings based on administrative boundaries and level of city urbanization. This study is based on the urban three-tier ring structure . All subdivided rings are normalized into standard circles and the administrative boundary or land cover/use type difference was not taken as the basis of circle division.

In the division of urban concentric ring pattern, the subdivided inner rings will divide the features. However, the ecosystem service depends heavily on the integrity of the ecosystem, which in turn depends on the integrity of features in the spatial distribution. The range of the features is calculated by the minimum circumscribed circle, which can reduce the influence of the geometric shape of the feature on the feature range. It can also denote feature size because the geometric direction of the features is ignored, and the feature will permanently reside inside its minimum circumscribed circle. To ensure the minimum land cover/use factor partitioning in the regional processing of circles, we measured the minimum circumscribed circle diameter (D_i) of features, and analyzed statistical characteristics of D_i. The subdivided rings are divided equidistantly by the 75th percentile of D_i.

2.4.3. The Boundary between Carbon Sequestration Eco-Service Zone and Carbon Emission Zone

For cities with mono-centric structure, locations farther from the city have less human activity and less damage to ecology. Furthermore, carbon density changes gradually, without significant interruption, with distance. However, according to the atmosphere diffusion simulation model, the carbon concentration in air will decrease drastically as the distance from the city increases and there will be a significant boundary for carbon distribution. Thus, this study used that as the boundary between carbon sequestration eco-service zone and carbon emission zone.

2.4.4. The Boundary between Carbon Sequestration Eco-Service Zone and Stable Carbon Stock Zone

To obtain a sequence that can represent the carbon sequestration capacity in different concentric rings, we counted the sum of the C concentration in different concentric rings, using subdivided inner rings to divide carbon concentration data. The Kriging interpolation is applied on the sequence, and we chose a subdivided inner ring corresponding to the point where carbon stocks tend to be stable in the sequence as the boundary between carbon sequestration eco-service zone and stable carbon stock zone.

2.5. The Scenario Simulation

The focus of the scenario analysis was directed on the carbon sequestration zone (Figure 2, Zone II). Population growth and socio-economic policies have important impacts on land cover/use change. Since ecosystem services directly depend on the land use type, land-use changes will affect ecosystem services. The change from a high carbon density land cover/use type to a low carbon density land cover/use type is manifested as carbon emission, i.e., the reverse conversion to carbon sequestration. Population density and an imbalance in economic development directly affect the spatial difference of regional carbon sequestration capacity [55,56]. Highly urbanized areas have serious problems in the destruction of carbon sequestration resources, resulting in instability of carbon sequestration resources and poor carbon stocks [57]. The change of land cover/use types drives the change of ecosystem service status. There is a strong negative correlation between the integrated urbanization level and the total value of ecosystem services [58]. The impact of land cover/use change on ecosystem service

function is significant, and the change of forest land is the most significant component [59]. Changes of cultivated land and water area have important secondary effects [60].

One purpose of this paper was to reveal the impact of carbon sequestration on ecosystem services through potential land cover/use changes. Scenario analysis helped reveal the potential impacts of land cover/use/cover change, policy management, and forest management changes on future ecosystem service value, relationship and overall benefits [61].

Based on the existing land cover/use change data, we analyzed the change of carbon sequestration eco-service under the influence of policies, using scenario simulation. First, changes in land cover/use structure and carbon stocks were summarized in 2014 and 2016. Then, based on the changing pattern of land cover/use in the development of small- to medium-sized cities [62,63] and the actual development situation and policy design of Guang'an, three scenario design schemes, which are benchmark development scenario, scenario of increasing carbon sequestration capacity based on the warning limit of cultivated land ("red line") and scenario of increasing carbon sequestration capacity based on the ecological protection, were considered.

3. Results

3.1. The Spatial Distribution of Carbon Sequestration Eco-Service

3.1.1. Carbon Stocks

The parameters in Table 1, required by InVEST, are summarized from the literature [44–46] and existing remote sensing image classification data. We used ArcGIS to process the outcomes of InVEST to spatially express the carbon stocks of the study areas. Results across all Monte Carlo simulation runs were analyzed to produce the following data. In addition, variance of current carbon grassland is where most confident to occur sequestration.

The calculation results are shown with white and black stripes (Figure 3). White represents built-up areas with minimum values and black indicates forest areas with maximum carbon stock values. The north volume of the carbon stocks is greater than the carbon stock volumes of the south part. The larger carbon stock values distributed within specified distances occurred in a ring pattern. The carbon stock distribution of 2016 was similar to 2014 but one major change was the patch size and integrality of landscape elements. The patch of 2016 was larger and more complete, and the whole carbon stock increased by 2,297,880.254 T.

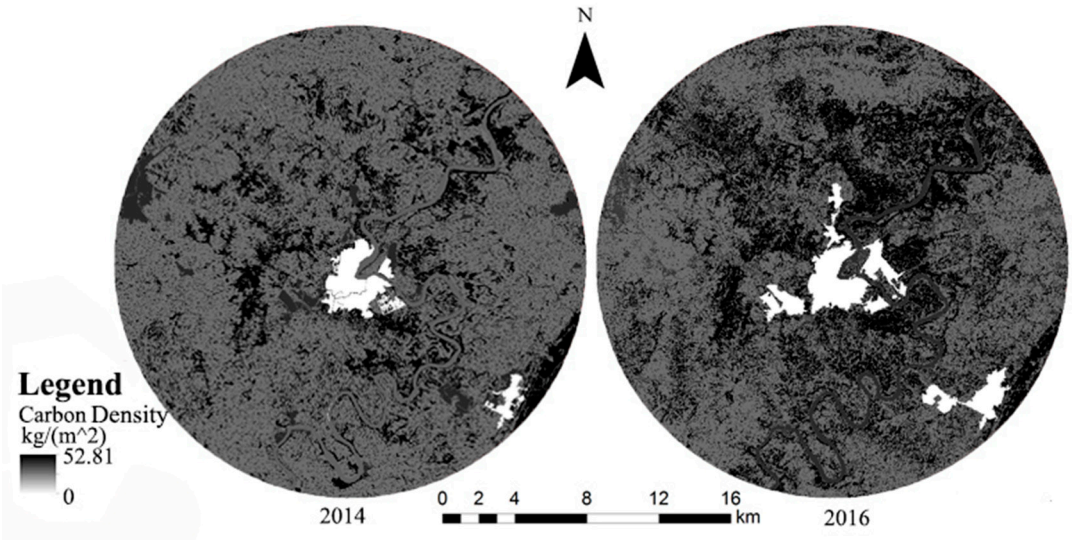

Figure 3. The distribution of carbon stocks in 2014, the distribution of carbon stocks in 2016.

Table 1. The carbon density of different land in four carbon pools (unit: Mg C ha^{-1}).

C_above_mean	C_above_sd	C_below_mean	C_below_sd	C_soil_mean	C_soil_sd	C_dead_mean	C_dead_sd	lucode	LULC_Name
0	0	0	0	0	0	0	0	1	City
94.1	4.7	121	6.1	233.4	11.1	0	0	2	Rural areas
2.3	1.2	145.4	7.3	200	10	0	0	3	Construction land
147	2.5	140.4	7	225.7	11.3	15	0.8	5	Forest land
35.3	1.7	6.5	3.3	406.9	20.4	1	0.5	8	Grassland
46.5	2.3	80.7	4	208.3	10.4	1	0.5	9	Cultivated land
27.75	1.4	112.7	5.6	213	10.5	1.23	0.6	10	Water body
21.7	1.1	34.4	1.7	371.8	18.1	0	0	11	Bare land

3.1.2. Macro Information of Carbon Stocks

Sampling for carbon stocks map could reduce the data volume, while the sampling result (Table 2) is reasonable and characteristic of the data required to obtain the spatial distribution of carbon density. There were 65,975 patches of different land cover/use in the study area; the maximum area was 177,075,900 m^2 and the minimum value was 900 m^2.

Table 2. Sampling result.

2014								
Lucc	**City**	**Cultivated Land**	**Construction Land**	**Water Body**	**Bare Land**	**Rural Areas**	**Grassland**	**Forest Land**
Sampling percentage	0.036	0.52	0.022	0.031	0.007	0.066	0.012	0.306
Actual percentage	0.020	0.604	0.018	0.051	0.007	0.145	0.002	0.152
2016								
Lucc	**City**	**Cultivated Land**	**Construction Land**	**Water Body**	**Bare Land**	**Rural Areas**	**Grassland**	**Forest Land**
Sampling percentage	0.024	0.614	0.022	0.061	0.01	0.12	0.001	0.148
Actual percentage	0.036	0.511	0.015	0.027	0.007	0.072	0.014	0.318

The sampling percentage of the land cover/use types is close to the actual percentage and can be used to reflect the ratio between the land cover/use types. Therefore, the sampling result is reasonable and can be used as a database to reduce the accuracy of carbon stocks. The features selected by area represent the features with large carbon stocks in the entire study area. We assigned the carbon stock value attribute of the features to the corresponding sample point features. Kriging interpolation of the sampling points provided a carbon density distribution. Due to random sampling when there is no sampling point around the border, the boundary based on interpolation does not coincide with the original boundary. There is the outer boundary of carbon sequestration zone and carbon density in 2016 (Figure 4).

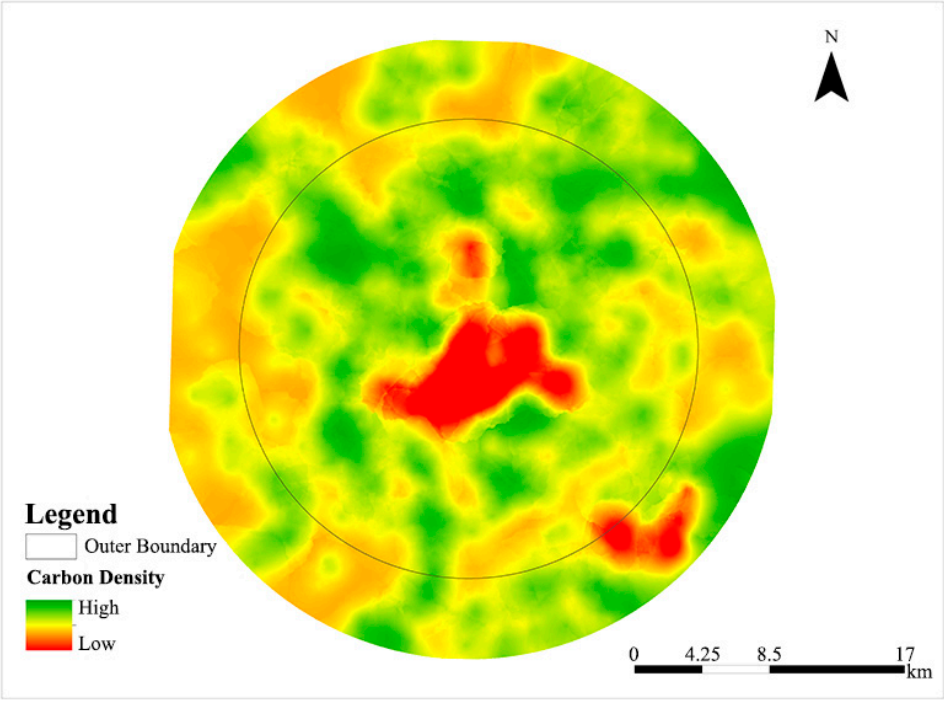

Figure 4. The outer boundary of carbon sequestration zone in 2016; that is, the boundary between carbon sequestration zone and stable carbon stock zone.

It can be seen in Figure 4 that the area with high carbon stocks within the outer boundary is around the city and the area beyond the outer boundary is stable region where the carbon stocks are stable. The spatial distribution is consistent with the assumption in this paper. Therefore, the assumption that the spatial distribution of carbon cycle follows the concentric ring pattern is established in Guang'an.

3.2. The Spatial Distribution of Carbon Emissions

In 2014, the energy consumption of Guang'an converted to standard coal was equivalent to 2.2299 million tons, and the 2016 value was about 1,675,460 tons. According to General Principles for Calculation of Total Production Energy Consumption, 10^{-3} Mg standard coal in the case of complete oxidation will produce about 2.83×10^{-3} Mg CO_2, generating C emissions of about 7.72×10^{-4} Mg. Total carbon emissions over the two years was approximately 3,905,360 tons, so about 1,607,479 tons of carbon was not absorbed, and the absorption of city carbon emission was about 58.84% in the suburbs.

The density of urban POI was taken as the substitution point of urban carbon source, and the density of POI was calculated by the point density tool in ArcGIS (Figure 5).

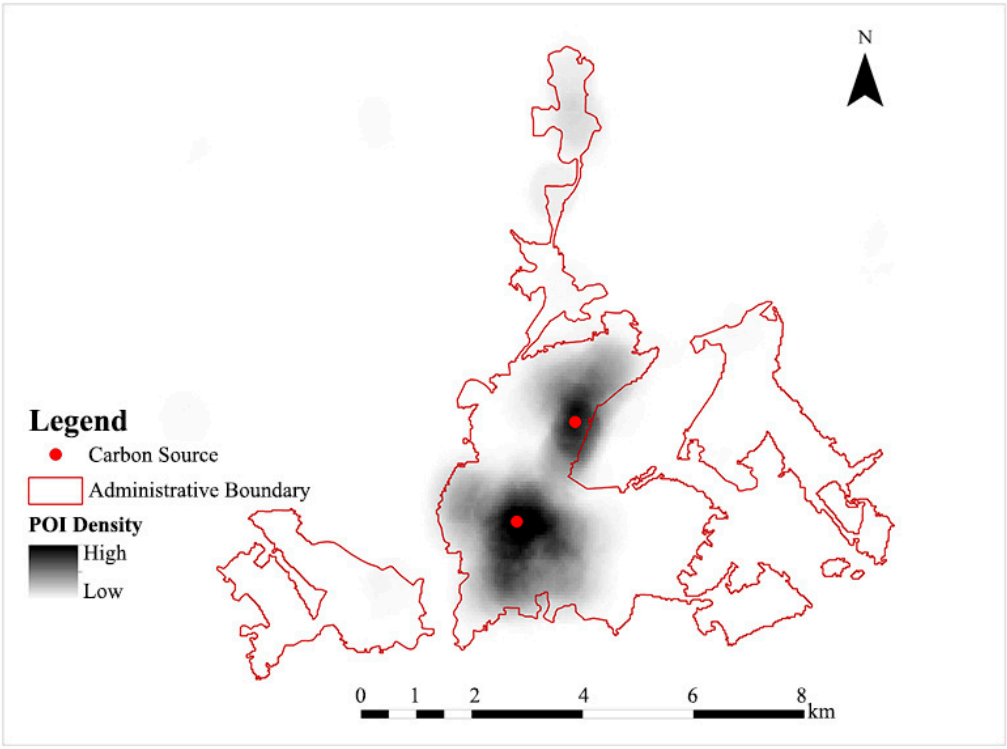

Figure 5. Substitute carbon sources in city.

There were two peaks in the spatial distribution of POI density, so there were two substitute carbon sources (Figure 5). The north carbon source coordinates were 106°38′20.244″ E, 30°28′50.937″ N and the southern carbon source coordinates were 106°37′39.534″ E, 30°27′49.573″ N. The POI density value was divided into upper and lower parts. The sum of the grid values of each part was counted, and the urban carbon emission was distributed proportionally to each carbon source. The carbon source in the north accounted for 33.24% of the total carbon in 2014, while the southern part accounted for 66.76%. In 2016, the carbon source in the northern part accounted for 29.86% of the total, while the carbon source in the southern part accounted for 70.14%. The P-G parameters and the emission rates of the northern and southern carbon sources were introduced into the modified static wind Gaussian diffusion model (Equation (4)), and we calculated the carbon concentration at different distances from the carbon sources. The results are shown in Tables 3 and 4.

Table 3. Spatial distribution of carbon concentrations at different distances of carbon sources in 2014.

Distance (km)		0.1	0.2	0.3	0.4	0.5	0.6	0.8	1
Concentration (g/m^3)	Northern carbon source	7.29	1.97	0.91	0.53	0.34	0.24	0.14	0.09
	Southern carbon source	14.67	3.97	1.84	1.07	0.69	0.49	0.29	0.19
Distance (km)		1.2	1.4	1.6	1.8	2	3	4	6
Concentration (g/m^3)	Northern carbon source	0.07	0.05	0.05	0.03	0.03	0.01	0.01	0.00
	Southern carbon source	0.13	0.10	0.10	0.06	0.05	0.02	0.01	0.01

Table 4. Spatial distribution of carbon concentrations at different distances of carbon sources in 2016.

Distance (km)		0.1	0.2	0.3	0.4	0.5	0.6	0.8	1
Concentration (g/m^3)	Northern carbon source	4.93	1.33	0.62	0.36	0.23	0.17	0.10	0.06
	Southern carbon source	11.57	3.13	1.45	0.84	0.55	0.39	0.23	0.15
Distance (km)		1.2	1.4	1.6	1.8	2	3	4	6
Concentration (g/m^3)	Northern carbon source	0.04	0.03	0.03	0.02	0.02	0.01	0.00	0.00
	Southern carbon source	0.10	0.08	0.08	0.05	0.04	0.02	0.01	0.01

The buffer radius was set according to the P-G parameter with each carbon source as the center to form a multi-ring buffer. The above values were assigned to the buffer in the form of attributes, and then by spatial stacking to obtain a spatial distribution of carbon emission concentration (Figure 6).

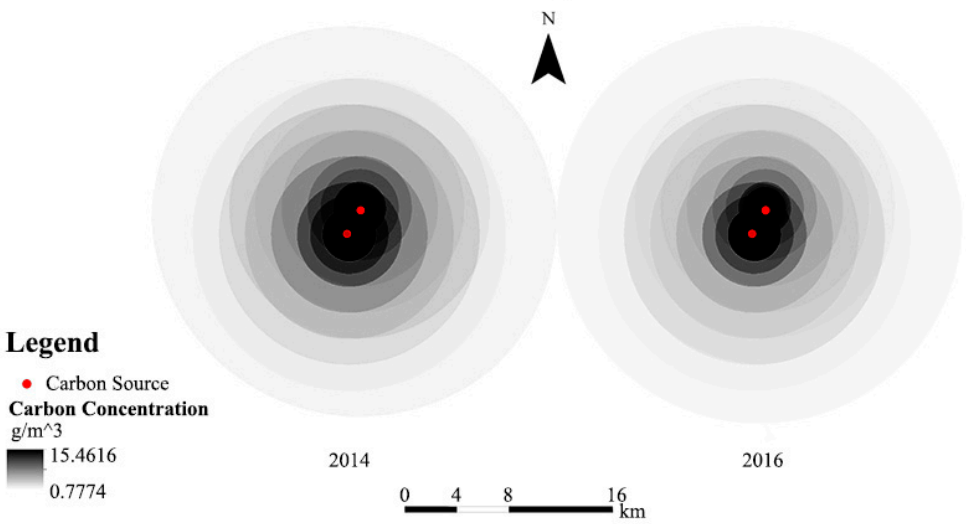

Figure 6. The spatial distribution of carbon concentration.

To clarify the difference in C concentration distribution, we sampled the existing concentration distribution results on the axis of the alternative carbon source and the vertical bisector. The sampling points and the sampling results are shown as Figure 7.

3.3. The Spatial Distribution of Carbon Cycle

3.3.1. The Subdivided Inner Rings

Minimum circumscribed circle of features was obtained with the "Minimum Bounding Geometry" tool in ArcGis. The output layer attribute table was exported as a dbf file, and then to the statistical functions (AVERAGE and QUARTILE) of Excel to determine features (Table 5).

Table 5. The characteristic of land cover/use patches size in 2014 and 2016.

Year	Minimum (Unit: m)	Maximum (Unit: m)	75th Percentile (Unit: m)
2014	42	8961	1172
2016	67	8723	1275

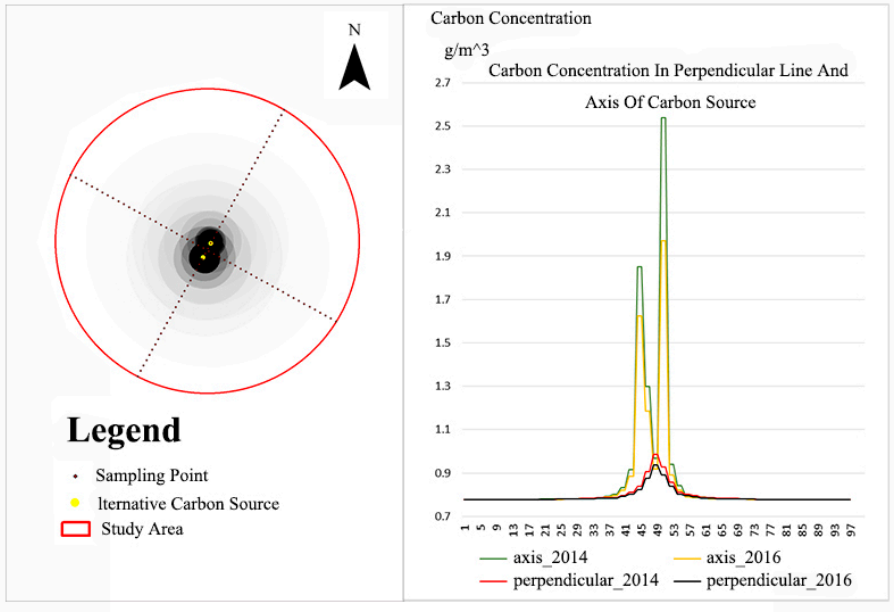

Figure 7. The sampling points and the sampling results.

The outermost circle (Figure 1) coincides with the boundary of the study area, with the 75th percentile of DI as the spacing between the circles, from the edge of the study area to the city feature gravity dividing the circles. The "MultipleRingBuffer" tool of ArcGis was used to form 17 circles in 2014 data, and 16 circles in 2016 data (Figure 8).

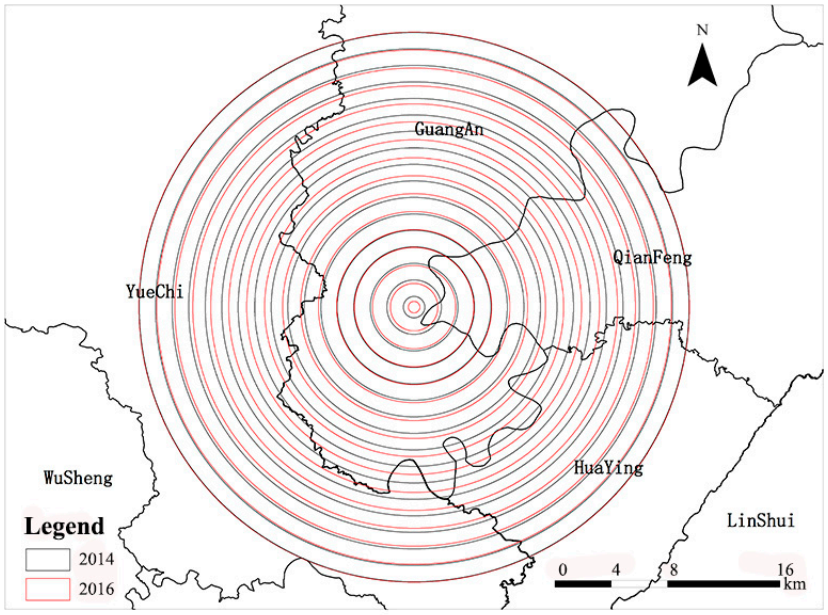

Figure 8. The subdivided inner rings diagram. Red represents subdivided inner rings in 2016 and blue represents subdivided inner rings in 2014.

3.3.2. The Boundary between Carbon Sequestration Eco-Service Zone and Stable Carbon Stock Zone

Using the 2016 data as an example, we obtained the change of carbon density in different subdivided inner rings (Figure 9).

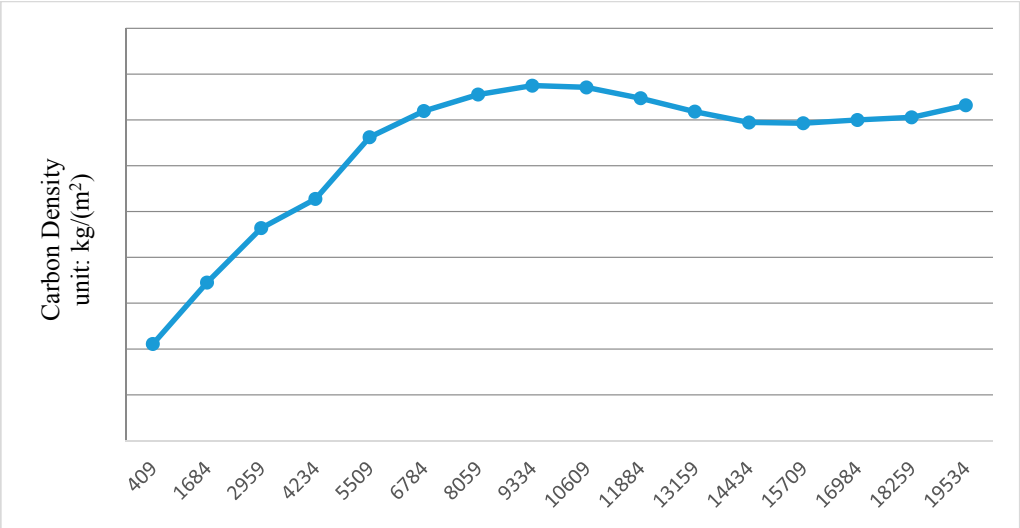

Figure 9. Carbon density in different rings.

The carbon density was lowest when the radius of the ring was 15,072 m. Therefore, the radius of the subdivided inner ring, which is the boundary between carbon sequestration eco-service zone and stable carbon stock zone, is 15,072 m.

3.3.3. The Boundary between Carbon Sequestration Eco-Service Zone and Carbon Emission Zone

After urban carbon emission concentration numerical histogram equalization, we obtained a discrete point distribution of each concentration value (Figure 10).

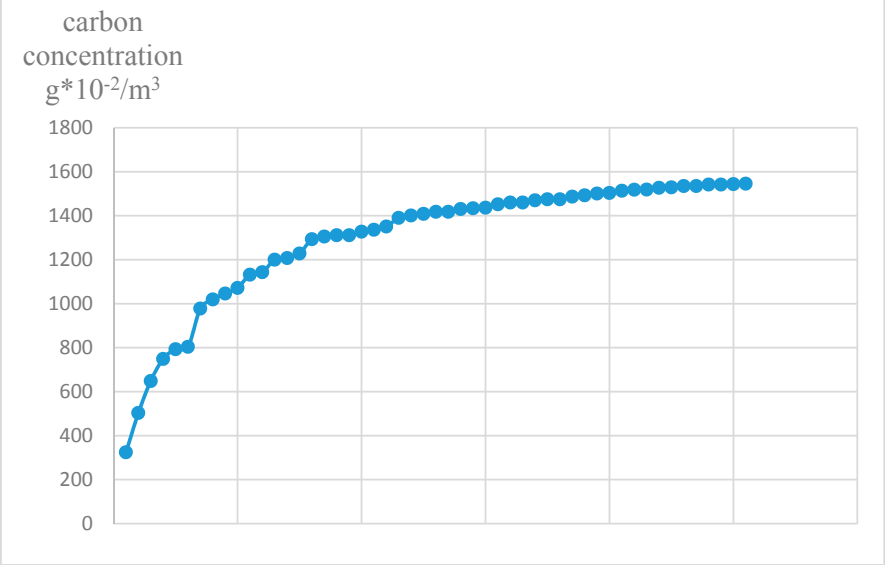

Figure 10. Discrete point of each concentration value.

According to the modified atmospheric diffusion model, the larger values of C concentration are mainly distributed in the region close to the carbon source, and the values decrease with increasing distance. In the region with low value, there were many pixels and the contrast was low. When histogram equalization was carried out in the spatial domain, the gray value of the image was extended between gray levels of 0 to 255 to display the image contrast and improve image quality, and simplify the algorithm [64]. To enhance low-value area contrast and increase visibility of the C concentration boundary, we stretched the results of spatial distribution of C concentration using histogram equalization. We chose the subdivided inner ring where the gray values change slowly for the boundary between carbon sequestration eco-service zone and carbon emission zone. Therefore, in Figure 9, the subdivided inner ring whose carbon concentration value is 8.03 g/m^3 is the boundary, the original concentration is 0.87 g/m^3, and the radius of the ring is 6351 m.

3.3.4. The Spatial Distribution of Carbon Cycle

In summary, the 2016 carbon sequestration zone in Guang'an City is defined as an annular region 6351–15,072 m from the city center. In 2014, the carbon sequestration zone is defined as an annular region 6623–14,827 m from the city center(Figure 11). In 2016, the carbon density in the carbon sequestration zone was 417.2 Mg C ha^{-1}, while, in 2014, it was 392.1 Mg C ha^{-1}.

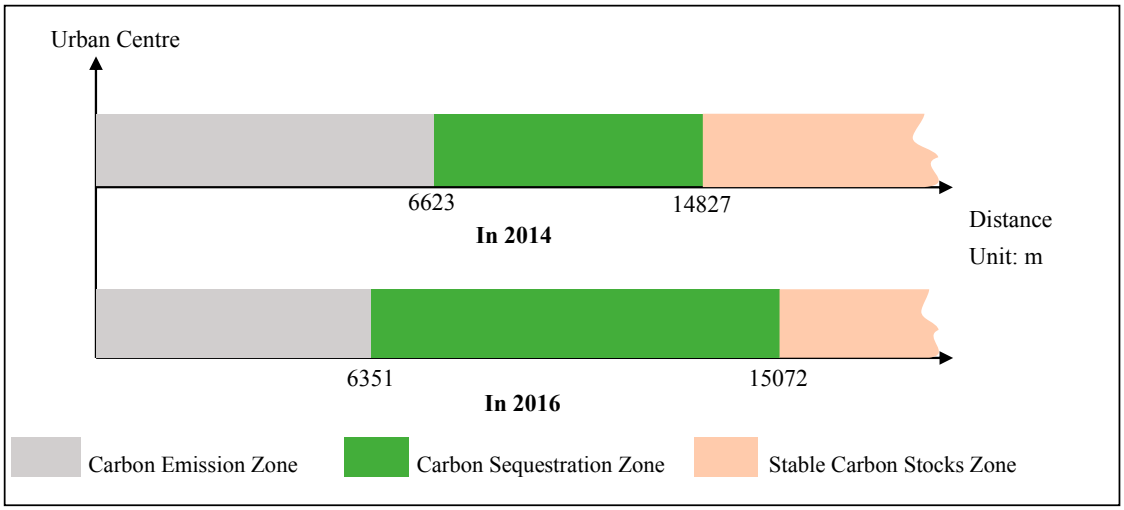

Figure 11. The spatial distribution of carbon cycle in Guang'an.

3.4. The Scenario Simulation

3.4.1. Land Cover/Use Changes and Carbon Stocks Changes

The land cover/use change in the carbon sequestration zone was analyzed for two years. The land cover/use classification layers in 2014 and 2016 were divided using the ecological service zone, and the carbon stocks of different land cover/use types were updated and estimated by the Build Raster Attribute Table in ArcGIS. In 2016, the total area of the carbon sequestration zone increased by 6683.94 ha compared to 2014. The changes of land cover/use types are shown in Table 6.

In Table 6, the land cover/use type that changed most in the carbon sequestration zone was forest land, which was mainly transformed from cultivated and rural land. In Guang'an, urban expansion occurred after 2014 when a large proportion of the rural population moved into the city and increased the population density. Following this immigration, the Government implemented a policy of returning farmland to forests that resulted in a reduction of rural land around the city and an increase in forest land. Different land cover/use types have different carbon sequestration capacities, and carbon stock changes were caused by changes of land cover/use in the carbon sequestration zone.

The increase in carbon stocks in 2016 compared with 2014 was 4023.50382 kilotons (kt), with increased forest land making a major contribution to the increase in carbon stocks (Table 7).

Table 6. Land cover/use change in carbon sequestration zone.

Land Cover/Use Types	2014 (ha)	2016 (ha)	Change (ha)
City	15	556	541
Cultivated land	28,715	26,399	−2316
Construction land	923	652	−271
Water body	2594	1993	−601
Bare land	476	783	307
Rural areas	6425	2982	−3443
Grassland	61	837	776
Forest land	9989	21,680	11,691

Table 7. Carbon stocks change in the carbon sequestration zone.

Land Cover/Use Types	2014 (kt)	2016 (kt)	Change (kt)
City	0	0	0
Cultivated land	9662.43	8883.11	−779.32
Construction land	320.82	226.78	−94.04
Water body	919.86	706.74	−213.12
Bare land	203.65	334.97	131.32
Rural areas	2881.70	1337.62	−1544.08
Grassland	27.32	376.24	348.92
Forest land	5275.24	11,449.07	6173.83

3.4.2. Scenarios Design

Benchmark development scenario (Scenario 1): Consistent with land cover/use constraints under current planning conditions and socio-economic development, we make the following projections: the amount of urban carbon emissions will remain unchanged; the inner radius of the carbon sequestration zone will be unchanged; and the rate of expansion of the outer radius and the rate of change of the various types of soil utilization in the zone will not change.

Scenario of increasing carbon sequestration capacity based on the warning limit of cultivated land ("red line") (Scenario 2): Basic farmland protection currently restrains the conversion of cultivated land to other land cover/use types. According to the "Plan of Land and Resources Management in Guang'an City" (2016–2020) during the "13th Five-Year Plan" period, the "red line" of cultivated land and other government policies on cultivated land protection, the government has ordered "strict protection of cultivated land and basic farmland". Cultivated land will remain stable at 288,900 ha with a basic farmland protection area of not less than 248,100 ha. The surrounding cities and the surrounding county where the town and the traffic allows easy occupation of high-quality farmland is classified as permanent prime farmland. The 1600 ha of new cultivated land ensure that city construction projects are balanced by land conservation. Based on the "red line" of cultivated land, the reduction rate of cultivated land area was reduced and the quantity of cultivated land within the zone was equal to the red line of cultivated land. Slowing the growth of forest land and reducing the fragmentation of landscape as principle, the size of the zone was unchanged. The changes of land cover/use are mainly in cultivated land and woodland. According to the ratio of the area of the zone to the area under the jurisdiction of the city, we determined that the area of cultivated land within the zone should not be less than 24,335 ha by 2020.

Scenario of increasing carbon sequestration capacity based on the ecological protection (Scenario 3) strengthens the protection of ecological land, such as woodland, grassland and water areas, while accelerating the transformation of unused land to ecological land. Guang'an is located in hilly country and major ecological problems involve soil erosion and water loss. The demand for forest land under

ecological protection can reach 44% of the study area [65,66]. In the north of the study area, forest land change is the most obvious. Therefore, in the northern forest lands, especially the state-owned forest lands, measures such as closing hillsides to facilitate afforestation were adopted. Currently, the rate of expansion of the outer boundary of the carbon sequestration zone remains constant. The bare land area is maintained at the 2016 level and the grassland is growing at a rate of forest change, with a forest cover of 44%.

In combination with the data calculations and the actual situation in Guang'an, the key factors were identified as: (1) size of the carbon sequestration zone (based on the data from 2014 to 2016, the growth rate of the carbon sequestration zone area is 3341.97 ha year^{-1}); and (2) the proportion of the different types of land cover/use under different scenarios (Table 8).

Table 8. The proportion of the area of different land cover/use types in three development scenarios.

Key Factors	Scenario 1	Scenario 2	Scenario 3
Size of carbon sequestration zone	69,249 ha	62,565 ha	69,249 ha
City (proportion)	0.99%	0.99%	0.99%
Cultivated land (proportion)	47.24%	43.55%	42.10%
Construction land (proportion)	1.17%	1.17%	1.17%
Water body (proportion)	3.57%	3.57%	3.57%
Bare land (proportion)	1.40%	1.40%	1.13%
Rural areas (proportion)	5.34%	5.34%	5.34%
Grassland (proportion)	1.60%	1.50%	1.70%
Forest land (proportion)	38.70%	42.49%	44.00%

3.4.3. The Influences on Carbon Sequestration in Different Scenarios

The design of scenarios takes into account benchmark development, "red line" policy, and ecological protection. According to the scenario design, the carbon sequestration zone experiences expected growth rate of 3341.97 ha year^{-1}. To clarify the difference of different scenarios, we discuss the land cover/use in 2020 according to the "Plan of Land and Resources Management in Guang'an City" (2016–2020), when the total area will be 69,248.88 ha. The land cover/use structure of different scenario simulation method by 2020 is shown in Table 9. Using the carbon density of different land cover/use types, the carbon stocks of the carbon sequestration zone in different scenarios and the changes of carbon density compared with 2016 were calculated (Table 10).

Table 9. Different scenarios of land cover/use types in 2020.

Land Cover/Use Types	Scenario 1 (ha)	Scenario 2 (ha)	Scenario 3 (ha)
City	688	556	688
Cultivated land	32,714	24,335	29,158
Construction land	808	652	808
Water body	2470	1993	2470
Bare land	970	783	783
Rural areas	3696	2982	3696
Grassland	1037	837	1176
Forest land	26,866	23,743	30,470

Table 10. Change of carbon sequestration capacity in different scenarios in 2020.

	Scenario 1	Scenario 2	Scenario 3
The total of carbon stocks (thousand tons)	28,892.02	23,710.04	29,581.08
The changes of carbon density (Mg C ha^{-1})	0	+7.1	+10

In the three scenarios, forest land in the ecological protection scenario occupies 44%, the cultivated land protection scenario accounts for 42.5%, and the baseline development scenario takes up 38.8%. Although the total carbon stocks in the cultivated land protection scenario are the lowest, the carbon density ranks second to ecological protection scenario because of a higher proportion of forest land than the other scenarios. In the benchmark development scenario, carbon sequestration capacity was significantly less than the other two scenarios, even though the carbon sequestration zone expanded. This may indicate that the current development of the ecological service function is not the best condition. The proportion of cultivated land in the benchmark development scenario is higher than the other two scenarios, but this has weakened the ecological service capacity of the carbon sequestration. The carbon sequestration capacity of cultivated land protection scenario is better, and the level of cultivated land is in balance with the policy requirement for cultivated land. In the ecological protection scenario, the carbon sequestration capacity is the strongest, but the conversion of cultivated land is too great, which is lower than policy demands. Considering the protection of cultivated land and the protection of ecology, the cultivated land protection scenario appears to be the best choice.

4. Discussion

In this paper, the concentric ring theory and the mono-centric model are used to study the spatial distribution of the carbon cycle in mono-centric cities and suburbs. The results show that the spatial distribution of the carbon cycle in Guang'an follows the concentric ring pattern. Our conclusion is consistent with the concentric ecological model proposed by Li, combined with the concentric ring theory. Our results agree that the ecosystem had a concentric ring distribution with the city at the center [67]. Through discussing the influence that regulation of the carbon sequestration zone and land cover/use has on the carbon sequestration capacity of the city, we conclude that it is significant for formulating land cover/use policies that maintain the carbon cycle stability of cities.

We analyzed the results and concluded that the government's afforestation policy is a direct factor in the expansion of the carbon sequestration service zone. Forested land in the study area increased by nearly 12,000 ha over a two-year period, partly due to the government policy of returning farmland to forests. Forests are primary carbon absorbers, and the carbon sequestration function of plantation forests can help mitigate global climate change [68,69]. Some scholars have also come to a similar conclusion; that is, an important factor in the change of carbon sequestration eco-services is that the government reduces ecological land area to increase construction land area [70–72]. Our results also verify the conclusions of these scholars. Based on the land use policy, we also discuss the impact of energy consumption on the spatial distribution of the carbon cycle. Under the environment of emissions reduction policy, the goals of structural and project emissions reduction have been achieved. These policies helped to reduce the total emissions of the province [73]. The results of the carbon sequestration zone evaluation indicate that government policy has not changed the structure of the concentric ring, but the original carbon sequestration zone has widened. Afforestation and forest restoration can increase the carbon sequestration function as well as promote water conservation, climate regulation, and resource supply. The absorption rate of urban carbon emissions in Guang'an was 58.84%. The "China Greenhouse Gases Bulletin in 2013" noted that about 55% of CO_2 is absorbed by the biosphere and ocean around China, so the absorption rate exceeds this average. The C absorption rate in Guang'an is higher than the national average.

The spatial distribution of the carbon sequestration zone results from the influence of both human activities and natural phenomena. The results of carbon stocks show that forested land is distributed between the city and a large area of cultivated land in the form of a ring because of human activities, urban expansion, and the reclamation of cultivated land. According to the spatial distribution of carbon stocks (Figure 2), the carbon sequestration in the north of the city is larger than that in the south, and this is closely related to the southerly and northerly wind directions. Southerly winds predominate in Guang'an, accounting for about 85.67% of the region's winds [74]. This is subject to further analysis in future research.

China is currently promoting the concept of urban ecosystem services, and urban managers are trying to plan more compact and sustainable cities through urban eco-spatial division and land cover/use change. Based on scenario analysis, the benchmark development scenario was not the best development mode. The different scenarios included different land cover/use structures with the main differences being the proportion of forest land, grassland and cultivated land. The benchmark development scenario trend showed that the proportion of cultivated land in the carbon sequestration zone was the highest, accounting for 47.24% of the area of the area, reducing the coverage of forest land and weakening the carbon sequestration capacity compared to the ecological protection scenarios. With the ecological protection scenario, forest coverage could reach 44%, the carbon sequestration capacity is the strongest, and the carbon stock per square meter was 4.27×10^{-2} Mg. Compared with the benchmark development scenario, carbon density increased by 10 Mg C ha^{-1}, but, in the carbon sequestration zone, the proportion of cultivated land was lower than the minimum required by government policy. In the cultivated land protection scenario, the size of the ring was unchanged but the internal land cover/use was more balanced. The carbon sequestration capacity improved compared to that in the benchmark development scenario, increasing by 7.1 Mg C ha^{-1}, and the amount of cultivated land was maintained within the range required by government policy, which promised to meet the requirements of food supplying. To maximize the amount of carbon stocks, both ecological protection and human economic activities should be considered [75]. We cannot blindly change non-ecological lands to ecological land. The sustainable carbon balance is a natural and social combination system. The carbon sequestration capacity of adjacent areas is changed due to these mutual influences, so we should strengthen the spatial link. This allows regions with strong carbon sequestration capacity to spread their ecological effects and improve regions with weak carbon sequestration capacity [76]. Our scenario simulation results verify the correctness of the view that reasonable land use policy to maintain the stability between human well-being and ecosystem is necessary. Reasonable adjustment of land cover/use structure and spatial distribution is necessary to ensure ecological and economic stability and to achieve the sustained change of urban structure and function. Calthorpe, a famous urban planning scholar, pointedly observed that sustainability is to seek a balance among the social, economic and ecological environment, so that it can exist forever [77]. Therefore, to achieve the changes that urban scale (population, land, and production) is getting bigger, urban structure is gradually coordinated and urban function is gradually sustainable, urban sustainable development at a certain time and space scale, through long-term sustainable urban growth and its structural evolution, is necessary to not only meet the needs of contemporary reality, but also to meet the requirements of future development. In terms of the sustainable development of Guang'an, the planning of urban eco-service spatial patterns and land cover/use should take the protection of cultivated, protection of ecological areas and the functional requirements of urban development into consideration at the same time.

Many cities have developed from the mono-centric model, not only in China, but also in other world regions [78,79]. Many cities have a multi-centric spatial structure developed from a mono-centric structure. For example, in Seoul, its urban spatial structure in the 1880s was a typical mono-centric pattern with only one central business district [80]. The mono-centric model is still considered an important theory that can describe the spatial structure of cities [81]. We consider urban structure, development mode, carbon sequestration capacity, and the assessment value of carbon emissions, thus our conclusions have high application value to the sustainable development of Guang'an, and a certain reference value for the spatial distribution of carbon cycle of other cities with similar structure to Guang'an. The results have application value and guiding significance for the planning of mono-centric cities. We can identify and delimit the carbon sequestration functional area in the city according to land cover/use data and urban carbon emission data. Whether, and how, this can be applied to complex urban structure areas are subjects for further study.

Further studies should focus on three areas: First, there should be improved selection and correction of data. The method used for calculating the spatial distribution of carbon sequestration

capacity and carbon emissions should also be improved. For example, this paper did not consider the relative carbon sequestration capacity strength of land cover/use patches in a city. An improved InVEST model with this consideration would better reflect the demand and supply values of the city. The accuracy of the estimated spatial distribution of carbon emission concentrations is insufficient and this reduced the computational accuracy of the inner boundary of the carbon sequestration zone. Similarly, the lack of an accurate classification of woodland areas reduced the computational accuracy of carbon stocks. Accurate determination of urban and peripheral CO_2 concentrations will be the focus of a follow-up study. Second, the changing laws of carbon sequestration zone and the effects on carbon sequestration should consider land cover/use as well as the natural environment (e.g., wind speed and wind direction), urban construction and development needs, and production factors. Integration of a set of programs able to solve multiple questions and balance the ecological service and the reasonable use of land will be the goal of additional studies. Third, a discussion of the carbon sequestration zone of the multi-centric city merits further study because, in addition to Guang'an and other fourth-tier cities, the second- and third- tier cities of China are mostly multi-centric cities.

5. Conclusions

This paper discussed the spatial distribution of carbon cycle for mono-centric cities, based on the von Thünen concentric ring theory, using an integration of the InVEST model and the revised atmospheric diffusion model, combined with land cover/use, carbon emissions and ecological data, and we discuss the various factors of land cover/use change on urban carbon cycle and its spatial pattern evolution using scenario simulations. This analysis provides a basis for effective planning and using of urban land. The results show that:

(1) Carbon sequestration and carbon emissions in the mono-centric cities follow a concentric ring pattern. The first annular zone (Zone I) represents the carbon emissions, which lie at the concentric ring center; the second annular zone (Zone II) represents the carbon sequestration service; and the third annular zone (Zone III) represents stable carbon stock. From the view of supply and demand, combined with carbon emissions and carbon sequestration capacity data through identification and delimitation of carbon sequestration zone in the mono-centric cities, this paper provides evidence for the government carrying out ecological environment assessment and planning.

(2) In the study area, the carbon sequestration zone is an annular region 6623–14,827 m from the city center in 2014, and an annular region 6351–15,072 m from the city center in 2016. The structure of the concentric ring has not changed, but the spatial distribution of carbon sequestration and carbon density has changed due to fossil energy consumption and land cover/use change. Compared with 2014, the carbon emission zone shrunk while the carbon sequestration service zone expanded in 2016.

(3) The eco-service capacity of the carbon sequestration zone relates to the spatial division and different land cover/use types. In 2016, the carbon density of in the carbon sequestration zone was 417.2 Mg C ha^{-1}, compared with 392.1 Mg C ha^{-1} in 2014. It had obviously increased. Compared with 2014, the carbon stocks in 2016 increased by 4023.50382 thousand tons (kt), and this is the main factor of the forest land area increasing. This conclusion coincides with the actual situation of Guang'an. Urban green cover from 2014 to 2016 increased by 12,000 ha, which is closely related to government in Guang'an implementing the policy of returning farmland to forest.

Based on the urban land-use and eco-service time variation simulation, it is found that the current carbon-sequestration eco-service in Guang'an is not the best development condition. Under the ecological protection scenario, the carbon sequestration capacity is the strongest, but the conversion of cultivated land is too great, which is lower than policy demands. Under the cultivated land protection scenario, the government constrains the conversion of cultivated land to other land cover/use types. Although the total carbon stocks are the lowest, the carbon density ranks second to ecological protection

scenario because of a higher proportion of forest land than the other scenarios. Under the benchmark development scenario, carbon sequestration capacity was significantly less than the other two scenarios, even though the carbon sequestration zone expanded. Therefore, the function of urban eco-services and its influence factors of change are important components of urban sustainable development. To achieve the sustainability of Guang'an, the planning of urban eco-service spatial patterns and land cover/use should consider the protection of cultivated and ecological areas at the same time. It is possible to provide ideas for coordinating and solving the eco-service, cultivated land protection, urban constructions and other issues through spatial planning and policy guidance in the land-use circle. In Guang'an, there was a positive correlation between the carbon sequestration capacity and the forest coverage of the carbon sequestration zone, with higher forest coverage leading to greater carbon sequestration capacity. There remains a need to rationally allocate the proportion of different types of land cover/use to ensure a balance among ecological services such as carbon sequestration and food supply, and to coordinate sustainable development of urban eco-service, cultivated land protection, and urban construction.

The research method of this paper can be used in other carbon cycle spatial studies of mono-centric cities, and has the flexibility to use different data sources. Data source and processing accuracy will improve in the future. If high-resolution remote sensing data and other environmental data become more readily available, the research of spatial distribution of carbon cycle nad land-use planning in urban ecological zone will be more rational.

Acknowledgments: This work was supported by the National Natural Science Foundation of China: "Remote Sensing Dynamic Monitoring Method of Vegetation Eco-Water and Water Stress in West Sichuan Plateau" (No. 41671432) and The Center Project of Urban Development Research of Resource–Based of Sichuan (No. ZYZX-YB-1405). The authors thank MDPI and LetPub (www.letpub.com) for its linguistic assistance during the preparation of this manuscript.

Author Contributions: All authors participated in the study. Zhigang Li, Jialong Zhong, Zishu Sun and Wunian Yang analyzed the data. Zhigang Li and Jialong Zhong lead the writing with assistance from Zishu Sun, with contributions from all authors.

Conflicts of Interest: The authors declare no conflict in interest.

References

1. Yin, K.; Lu, D.; Tian, Y.; Zhao, Q.; Yuan, C. Evaluation of carbon and oxygen balances in urban ecosystems using land use/land cover and statistical data. *Sustainability* **2014**, *7*, 195–221. [CrossRef]
2. Peters, G.P.; Weber, C.L.; Guan, D.; Hubacek, K. China's growing CO_2 emissions—A race between increasing consumption and efficiency gains. *Environ. Sci. Technol.* **2007**, *41*, 5939–5944. [CrossRef] [PubMed]
3. Alberti, M. Measuring urban sustainability. *Environ. Impact Assess. Rev.* **1996**, *16*, 381–424. [CrossRef]
4. Andersson, E. Urban landscapes and sustainable cities. *Ecol. Soc.* **2006**, *11*, 34. [CrossRef]
5. André, B.-L. Eco-polycentric urban systems: An ecological region perspective for network cities. *Challenges* **2012**, *3*, 1–42. [CrossRef]
6. Zhao, C.R.; Zhou, B.; Su, X. Evaluation of urban eco-security—A case study of Mianyang city, China. *Sustainability* **2014**, *6*, 2281–2299. [CrossRef]
7. Mi, N.; Hou, J.; Mi, W.; Song, N. Optimal spatial land-use allocation for limited development ecological zones based on the geographic information system and a genetic ant colony algorithm. *Int. J. Geogr. Inf. Sci.* **2015**, *29*, 1–20. [CrossRef]
8. Li, Y.; Lu, C.; Deng, O.; Chen, P. Ecological characteristics of china's key ecological function areas. *J. Resour. Ecol.* **2015**, *6*, 427–433. [CrossRef]
9. Manoratna, D.A.; Kawata, K.; Yoshida, Y. Environmental impact and travel time savings of a new monorail system in Colombo's commuting traffic. *Transp. Res. Part D Transp. Environ.* **2017**, *51*, 122–128. [CrossRef]
10. Li, T.; Burke, M.; Dodson, J. Transport impacts of government employment decentralization in an Australian city—Testing scenarios using transport simulation. *Socio-Econ. Plan. Sci.* **2017**, *58*, 63–71. [CrossRef]
11. Salvati, L.; Carlucci, M. Distance matters: Land consumption and the mono-centric model in two southern European cities. *Landsc. Urban Plan.* **2014**, *127*, 41–51. [CrossRef]

12. Rosser, J.B. Morphogenesis of Regional Systems. In *Complex Evolutionary Dynamics in Urban-Regional and Ecologic-Economic Systems*; Springer: New York, NY, USA, 2011; pp. 63–83.
13. VonThünen, J.H. *Der isolierte Staat in Beziehung auf Landwirtschaft und Nationalökonomie*; Neudruck nach der Ausgabe Letzter Hand (1842/1850); Fischer: Stuttgart, Germany, 1966; p. 687.
14. Kellerman, A. Agricultural location theory 1: Basic models. *Environ. Plan. A* **1989**, *21*, 1381–1396. [CrossRef]
15. Angelsen, A. *Forest Cover Change in Space and Time: Combining the Von Thunen and Forest Transition Theories*; Social Science Electronic Publishing: Rochester, NY, USA, 2007; pp. 1–43.
16. Kitsikopoulos, H. Urban Demand and Agrarian Productivity in Pre-Plague England: Reassessing the Relevancy of von Thunen's Model. *Agric. Hist.* **2003**, *77*, 482–522. [CrossRef]
17. Zhang, W.; Huang, B.; Luo, D. Effects of land use and transportation on carbon sources and carbon sinks: A case study in Shenzhen, China. *Landsc. Urban Plan.* **2014**, *122*, 175–185. [CrossRef]
18. Erb, K.H.; Fetzel, T.; Plutzar, C.; Kastner, T.; Lauk, C.; Mayer, A.; Niedertscheider, M.; Körner, C.; Haberl, H. Biomass turnover time in terrestrial ecosystems halved by land use. *Nat. Geosci.* **2016**, *9*, 674–678. [CrossRef]
19. Xu, Q.; Yang, R.; Dong, Y.X.; Liu, Y.X.; Qiu, L.R. The influence of rapid urbanization and land use changes on terrestrial carbon sources/sinks in Guangzhou, China. *Ecol. Indic.* **2016**, *70*, 304–316. [CrossRef]
20. Zhang, J.; Liu, C.; Hao, H.; Sun, L.; Qiao, Q.; Wang, H.; Ning, Y. Spatial-temporal change of carbon storage and carbon sink of grassland ecosystem in the three-river headwaters region based on modis GPP/NPP data. *Ecol. Environ. Sci.* **2015**. Available online: http://en.cnki.com.cn/Article_en/CJFDTotal-TRYJ201501002.htm (accessed on 22 August 2017).
21. Velasco, E.; Roth, M.; Norford, L.; Molina, L.T. Does urban vegetation enhance carbon sequestration? *Landsc. Urban Plan.* **2016**, *148*, 99–107. [CrossRef]
22. Tokimatsu, K.; Yasuoka, R.; Nishio, M. Global zero emissions scenarios: The role of biomass energy with carbon capture and storage by forested land use. *Appl. Energy* **2017**, *185*, 1899–1906. [CrossRef]
23. Mancebo, F.; Salles, S. Urban Agriculture: Fostering the Urban-Rural Continuum. *Chall. Sustain.* **2016**, *4*, 1–2. [CrossRef]
24. Hu, Y.; Zheng, Y.; Zheng, X. Simulation of land-use scenarios for Beijing using CLUE-S and Markov composite models. *Chin. Geogr. Sci.* **2013**, *23*, 92–100. [CrossRef]
25. Zhan, J.; Wu, F.; Shi, C.; Zhang, F.; Li, Z. Scenario Analyses of Land Use Conversion in the North China Plain: An Econometric Approach. *Adv. Meteorol.* **2013**, *2013*, 592121. [CrossRef]
26. Luo, J.; Zhan, J.; Lin, Y.; Zhao, C. An equilibrium analysis of the land use structure in the Yunnan Province, China. *Front. Earth Sci.* **2014**, *8*, 393–404. [CrossRef]
27. Sun, P.; Xu, Y.; Yu, Z.; Liu, Q.; Xie, B.; Liu, J. Scenario simulation and landscape pattern dynamic changes of land use in the Poverty Belt around Beijing and Tianjin: A case study of Zhangjiakou city, Hebei Province. *J. Geogr. Sci.* **2016**, *26*, 272–296. [CrossRef]
28. Wu, J.G. Urban ecology and sustainability: The state-of-the-science and future directions. *Landsc. Urban Plan.* **2014**, *125*, 209–221. [CrossRef]
29. Wu, J.G. Landscape sustainability science: Ecosystem services and human well-being in changing landscapes. *Landsc. Ecol.* **2013**, *28*, 999–1023. [CrossRef]
30. Wilson, M.; Wu, J. The problems of weak sustainability and associated indicators. *Int. J. Sustain. Dev. World Ecol.* **2017**, *24*, 44–51. [CrossRef]
31. Nassauer, J.I.; Raskin, J. Urban vacancy and land use legacies: A frontier for urban ecological research, design, and planning. *Landsc. Urban Plan.* **2014**, *125*, 245–253. [CrossRef]
32. Huang, L.; Wu, J.; Yan, L. Defining and measuring urban sustainability: A review of indicators. *Landsc. Ecol.* **2015**, *30*, 1175–1193. [CrossRef]
33. He, C.; Zhang, D.; Huang, Q.; Zhao, Y. Assessing the potential impacts of urban expansion on regional carbon storage by linking the LUSD-urban and InVEST models. *Environ. Model. Softw.* **2016**, *75*, 44–58. [CrossRef]
34. Azaria, D.E.; Lee, B.H.Y.; Troy, A.; Ventriss, C.; Voigt, B. Modeling the effects of an urban growth boundary on vehicle travel in a small metropolitan area. *Environ. Plan. B Plan. Des.* **2013**, *40*, 846–864. [CrossRef]
35. A Large-Scale Greening Meeting Was Held in Guang'an. Available online: http://www.scly.gov.cn/contentFile/201611/1479171271957.html (accessed on 12 May 2017).
36. Statistics Bulletin of Guang'an about National Economic and Social Development in 2015. Available online: http://www.gatj.gov.cn/html/sjfb/tjgb/16/04/1598-3.html (accessed on 25 May 2017).

37. National Data, National Bureau of Statistics of China. Available online: http://data.stats.gov.cn/easyquery.htm?cn=C01 (accessed on 25 May 2017).
38. Fregolent, L.; Vettoretto, L. Genesis of a Fluid Metropolitan Space. In *Post-Metropolitan Territories, Looking for a New Urbanity*, 5th ed.; Taylor & Francis: Henley-on-Thames, UK, 2017; pp. 75–94.
39. Tallis, H.; Polasky, S. Mapping and valuing ecosystem services as an approach for conservation and natural-resource management. *Ann. N. Y. Acad. Sci.* **2009**, *1162*, 265. [CrossRef] [PubMed]
40. Bai, Y.; Zhuang, C.; Ouyang, Z.; Zheng, H.; Jiang, B. Spatial characteristics between biodiversity and ecosystem services in a human-dominated watershed. *Ecol. Complex.* **2011**, *8*, 177–183. [CrossRef]
41. Nelson, E.; Mendoza, G.; Regetz, J.; Polasky, S.; Tallis, H.; Cameron, D.; Chan, K.; Daily, G.C.; Goldstein, J.; Kareiva, P.M.; Lonsdorf, E. Modeling multiple ecosystem services, biodiversity conservation, commodity production, and tradeoffs at landscape scales. *Front. Ecol. Environ.* **2009**, *7*, 4–11. [CrossRef]
42. InVEST Releases. Available online: http://data.naturalcapitalproject.org/invest-releases/ (accessed on 1 May 2017).
43. Geospatial Data Cloud. Available online: http://www.gscloud.cn/ (accessed on 12 April 2017).
44. Cantarello, E. Potential effects of future land-use change on regional carbon stocks in the UK. *Environ. Sci. Policy* **2011**, *14*, 40–52. [CrossRef]
45. Qiu, L.F.; Zhu, J.X.; Wang, K.; Hu, W. land use changes induced county-scale carbon consequences in southeast China 1979–2020, evidence from Fuyang, Zhejiang province. *Sustainability* **2015**, *8*, 38. [CrossRef]
46. Duarte, G.T.; Ribeiro, M.C.; Paglia, A.P. Ecosystem services modeling as a tool for defining priority areas for conservation. *PLoS ONE* **2016**, *11*, e0154573. [CrossRef] [PubMed]
47. Zhilin, L.; Zhou, Q. Integration of linear and areal hierarchies for continuous multi-scale representation of road networks. *Int. J. Geogr. Inf. Sci.* **2012**, *26*, 855–880. [CrossRef]
48. Wang, Y.; Li, X.; Gong, H. Ontology-based analysis of multi-scale modeling of geographical features. *Sci. China Technol. Sci.* **2006**, *49*, 121–131. [CrossRef]
49. Soytas, U.; Sari, R.; Ewing, B.T. Energy consumption, income, and carbon emissions in the United States. *Ecol. Econ.* **2007**, *62*, 482–489. [CrossRef]
50. Chen, G.; Wiedmann, T.; Hadjikakou, M.; Rowley, H. City Carbon Footprint Networks. *Energies* **2016**, *9*, 602. [CrossRef]
51. Zhang, R.Q. Theoretical derivation of the atmospheric diffusion model of a continuous volume source in conditions of light air and calm. *Environ. Monit. China* **1998**, *5*, 37–39.
52. Jiao, L.M.; Zhang, X. Characterizing Urban Expansion Of Main Metropolises In China Based On Built-up Densities in Concentric Rings. *Resour. Environ. Yangtze Basin* **2015**, *24*, 1721–1728.
53. Jiang, L.G.; Zhang, Z.L. Analysis on the ring structure of urban land use in Jinan city. *Areal Res. Dev.* **2005**, *4*, 2463–2466.
54. Feng, H.J.; Zhou, Z.X. Spatial differentiation of urban agricultural ecosystem services—A case study of Xi'an metropolitan zone. *Chin. J. Eco-Agric.* **2014**, *22*, 333–341. [CrossRef]
55. Sun, R.; Yuan, X.Z.; Liao, Z.J.; Cao, H. Dynamic and spatial pattern of forest carbon storage in chengyu economic region. *Res. Environ. Sci.* **2010**, *23*, 1456–1463.
56. Tao, L.I.; Yang, Z.J.; Gan, D.X.; Wang, Z.Y.; Chen, X.; Qi, Z.-X. Influence of changes in land use/cover on carbon effect in Chang-Zhu-Tan urban agglomeration. *J. Ecol. Rural Environ.* **2016**, *32*, 539–545.
57. Li, H.M.; Lu, F.; Tang, S.M.; Tang, L.J.; Wu, Q.H. Dynamic carbon sink of forests in Yuhang city with the development of urbanization. *J. Fudan Univ.* **2004**, *43*, 1044–1050. [CrossRef]
58. Bendor, T.K.; Spurlock, D.; Woodruff, S.C.; Olander, L. A research agenda for ecosystem services in American environmental and land use planning. *Cities* **2017**, *60*, 260–271. [CrossRef]
59. Li, H.; Li, Z.; Li, Z.; Yu, J.; Liu, B. Evaluation of ecosystem services: A case study in the middle reach of the Heihe River basin, Northwest China. *Phys. Chem. Earth Parts A/B/C* **2015**, *89–90*, 40–45. [CrossRef]
60. Ahmad, A.; Nizami, S.M. Carbon stocks of different land uses in the Kumrat valley, Hindu Kush Region of Pakistan. *J. For. Res.* **2015**, *26*, 57–64. [CrossRef]
61. Mörtberg, U.; Goldenberg, R.; Kalantari, Z.; Kordas, O.; Deal, B.; Balfors, B.; Cvetkovic, V. Integrating ecosystem services in the assessment of urban energy trajectories—A study of the Stockholm region. *Energy Policy* **2017**, *100*, 338–349. [CrossRef]
62. Han, S.S. Urban expansion in contemporary China: What can we learn from a small town? *Land Use Policy* **2010**, *27*, 780–787. [CrossRef]

63. Ferreira, J.A.; Condessa, B. Defining expansion areas in small urban settlements—An application to the municipality of tomar (Portugal). *Landsc. Urban Plan.* **2012**, *107*, 283–292. [CrossRef]
64. Fu, X.; Zeng, D.; Huang, Y.; Liao, Y.; Ding, X.; Paisley, J. A fusion-based enhancing method for weakly illuminated images. *Signal Process.* **2016**, *129*, 82–96. [CrossRef]
65. Hu, Y.-L.; Qi, R.-H.; You, W.H.; Da, L.-J. Ecological service functional assessment on forest ecological system of Kunshan city. *J. Nanjing For. Univ.* **2005**, *29*, 111–114.
66. Li, M.; Zhu, Z.; Vogelmann, J.E.; Xu, D.; Wen, W.; Liu, A. Characterizing fragmentation of the collective forests in southern China from Multitemporal Landsat imagery: A case study from Kecheng district of Zhejiang province. *Appl. Geogr.* **2011**, *31*, 1026–1035. [CrossRef]
67. Li, C. On the Confucian View of Nature Based on Ecological Ethics—Ecological Wisdom of Time-Dependent Mean and Ecological Mode of Concentric Circle. *J. Beijing Inst. Technol. (Soc. Sci. Ed.)* **2014**, *2*, 21.
68. Baral, H.; Guariguata, M.R.; Keenan, R.J. A proposed framework for assessing ecosystem goods and services from planted forests. *Ecosyst. Serv.* **2016**, *22*, 260–268. [CrossRef]
69. Yao, R.T.; Harrison, D.R.; Velarde, S.J.; Barry, L.E. Validation and enhancement of a spatial economic tool for assessing ecosystem services provided by planted forests. *For. Policy Econ.* **2016**, *72*, 122–131. [CrossRef]
70. Xiong, C.; Yang, D.; Huo, J.; Wang, G. Agricultural Net Carbon Effect and Agricultural Carbon Sink Compensation Mechanism in Hotan Prefecture, China. *Pol. J. Environ. Stud.* **2017**, *26*, 365–373. [CrossRef]
71. Fei, X.; Jin, Y.; Zhang, Y.; Sha, L.; Liu, Y.; Song, Q.; Zhou, W.; Liang, N.; Yu, G.; Zhang, L.; et al. Eddy covariance and biometric measurements show that a savanna ecosystem in Southwest China is a carbon sink. *Sci. Rep.* **2017**, *7*, 41025. [CrossRef] [PubMed]
72. Cavaleri, M.A.; Coble, A.P.; Ryan, M.G.; Bauerle, W.L.; Loescher, H.W.; Oberbauer, S.F. Tropical rainforest carbon sink declines during El Niño as a result of reduced photosynthesis and increased respiration rates. *New Phytol.* **2017**, *216*, 136–149. [CrossRef] [PubMed]
73. Guang'an Makes Remarkable Achievements on Overall Carbon Reductions During the 12th Five-Year Plan. Available online: http://www.guang-an.gov.cn/gasrmzfw/index.shtml (accessed on 26 August 2017).
74. Tianqi. Available online: http://lishi.tianqi.com/guangan/index.html (accessed on 26 August 2017).
75. Chen, D.D.; Deng, X.Z.; Jin, G.; Abdus, S.; Li, Z.H. Land-use-change induced dynamics of carbon stocks of the terrestrial ecosystem in Pakistan. *Phys. Chem. Earth* **2017**. [CrossRef]
76. Dawson, J.J.; Smith, P. Carbon losses from soil and its consequences for land-use management. *Sci. Total Environ.* **2007**, *382*, 165–190. [CrossRef] [PubMed]
77. Calthorpe, P.; Ryn, S.V. *Sustainable Communities: A New Design Synthesis for Cities, Suburbs and Towns*; Sierra Club Books: San Francisco, CA, USA, 1986.
78. Diao, L.L. Pattern Comparison and Characteristic Disparity of Urban Restructuring between Traditional Mono-centric City and Group City. *China Popul. Resour. Environ.* **2010**, *7*, 022.
79. Alpkokin, P.; Komiyama, N.; Takeshita, H.; Kato, H. Tokyo Metropolitan Area Employment Cluster Formation In Line With Its Extensive Rail Network. *J. East. Asia Soc. Transp. Stud.* **2007**, *7*, 1403–1416.
80. Sung, H.; Chang, G.C. The link between metropolitan planning and transit-oriented development: An examination of the Rosario Plan in 1980 for Seoul, South Korea. *Land Use Policy* **2017**, *63*, 514–522. [CrossRef]
81. Salvati, L.; Sabbi, A. Exploring long-term land cover changes in an urban region of southern Europe. *Int. J. Sustain. Dev. World Ecol.* **2011**, *18*, 273–282. [CrossRef]